Materials Research. 2020; 23(2): e20190605
DOI: https://doi.org/10.1590/1980-5373-MR-2019-0605

Effect of the Microstructure on the Wear Resistance of a Pearlitic Steel

A.P.G. Chaves[a], D.M.A. Centeno[a], M. Masoumi[b], H. Goldenstein[a]*

[a]*Universidade de São Paulo, Escola Politécnica, São Paulo, SP, Brasil*
[b]*Universidade Federal do ABC, Centro de Engenharia, Modelagem e Ciências Sociais Aplicadas, Santo André, SP, Brasil*

Received: November 01, 2019; Revised: April 02, 2020; Accepted: April 10, 2020

Despite the experimentation of bainitic and martensitic microstructures in wheel-rail steels, pearlitic microstructure remains dominant in railway track. The wear resistance behavior of bainitic and pearlitic microstructures is still a matter of controversy. In this study, pin-on-disc sliding wear tests were performed to analyze the effects of the microstructure on wear resistance. The AISI 1080 steel was isothermally treated at five temperatures using a dilatometer in order to obtain pearlite, bainite and martensite structures. After these treatments, bainitic and martensitic samples were tempered at 500°C. It was possible to achieve pearlitic specimens with interlamellar spacing ranging from 70 ± 4 nm to 243 ± 9 nm. It was found that the wear resistance increases with decreasing the interlamellar spacing, fine pearlite showed 30% lower mass loss than coarse pearlite. The severe deformation and dislocation accumulation in different depth from the contact surface were analyzed by electron backscattered diffraction technique. The results showed that the first 10 μm depth from the contact surface was severely deformed and a high number of random high-angle boundaries developed due to the large compressive force. Fine pearlitic structure tends to present a better wear performance when compared to bainitic or martensitic structures.

Keywords: *wheel-rail contact, pearlitic steel, sliding wear, pin-on-disc test, severe deformation, EBSD.*

1. Introduction

A nearly full pearlitic microstructure is widely used in wheel-rail steels railroad industry due to its strength and wear resistance characteristics. The strength of pearlite is highly depending on the spacing between cementite lamellae[1-3]. Some works showed that the reduction of the pearlite interlamellar spacing in steels can increase resistance to sliding wear[4-6].

The wear performance of bainitic steels still a controversy in studies. Some studies shows that the poor wear resistance of bainitic steels is justified due to the strong dependency on the transformations processing, which is related to the microstructure evolution. Some previous studies discussed that phases such as retained austenite, allotriomorphic ferrite[7], carbides[8], and/or martensite[9] could contribute to the poor wear resistance of bainitic steel. Furthermore, it was reported that deficient strain hardening ability might be considered another critical factor on the poor wear resistance[10-13]. In opposition, several studies have shown that bainitic steel has exceptional wear resistance[7,14,15]. In order to clarify this controversy, it is important to find or establish a microstructure - wear resistance relationship as a function of systematic comparison.

Continuous increases in per-axle load and in the train speed has compelled railway industries to improve their material. Wear of wheel/rail contact surface produces high cost, energy and time losses. Therefore, wear rate reduction is the one of railroad industry targets. Wear mechanisms are classified into two groups; adhesive and oxidative wear that generate during the steady state regime[16,17]. In general, a strong interaction of plastic deformation on wheel/rail contact leads to the adhesive wear, while the formation of oxides in surface contact decreases metallic contact and increases interfacial shear deformation resulting in the formation of wear debris. Lyu et al.[18] reported that adhesive wear mechanism is predominant on clean contact. However, oxidative wear is the primary wear mechanism in an open environment with high humidity. In general, the wear regime in materials is a complex phenomenon and depends on tribological and metallurgical systems variables.

The main objective of the present study is to show the influence of various pearlite interlamellar spacing obtained by isothermal treatments on sliding wear resistance and compare with other microstructures like a bainite and martensite. Electron backscattered diffraction (EBSD) analysis was carried in the transverse direction of one worn pin (700C sample) to show the distribution of induced deformation at different distances from the contact surface.

2. Experimental Procedures

2.1 Materials and heat treatments

A eutectoid steel with the chemical composition (Table 1) corresponded the class C AAR wheels was subjected to isothermal treatments which is shown in Figure 1. Each pin sample was machined with 4mm diameter and 10mm length

*e-mail: *anaengmecanica@gmail.com*

and all pin thermal treatments were carried out using a Bähr dilatometer model DIL805A.

To calculate the austenite critical temperatures (Ac1 and Acm) and martensite start temperature (Ms), according the ASTM A1033-04, some specimens were heated from the room temperature to 700°C with 10°C/s heating rate, and then continued to heat up to 780°C with 28°C/h heating rate. The samples were quenched with 150°C/s with Helium gas flow to ambient temperature.

In order to obtain different microstructures, the specimens were heat treated following the schematic representation showed in Figure 1. The samples were heated at 10°C/s from room temperature until 800°C and maintained at this temperature for 300s, then the samples were cooled at 150°C/s rate and isothermally treated at five different temperatures (700°C, 625°C, 550°C, 300°C and 50°C), two sample series (300CT and 50CT) were heated again until 500°C and tempered for 30 minutes, finally all samples were air cooled to ambient temperature.

2.2 Microstructure characterization

For microstructure characterization, the samples were ground and polished up to 1 µm diamond paste, and were etched by a 2% Nital solution. Then, samples were analyzed by a scanning electron microscope Inspect50 SEM-FEG. Microhardness tests were performed with HV0.1 using a durometer Shimadzu HMV-2TQDW.

To measure the pearlite interlamellar spacing, high resolution images from the SEM were analyzed. A scale line was drawn in a region with greater interlamellar spacing and it was counted how many times that line crossed a cementite lamella. Thus, the pearlite interlamellar spacing was estimated by dividing the scale line dimension by the number of intersections. Three images with minimum of five baselines of each sample were viewed.

2.3 Tribological tests

Wear test was performed using a pin-on-disc type model PLINT TE-79, according the ASTM G99-05. Five pins of each sample were tested against AISI H13 steel discs quenched and tempered to 600HV surface hardness. It is notable that the disc hardness always remains higher than pin hardness. A 10 N load was applied during sliding test. The sliding speed was 0.5m/s with 3600 seconds of test duration and five replicas for each microstructure were performed. Before each test, the surface pins were polished using 220 silicon carbide emery paper. The purpose of pin surface preparation was to ensure the same initial contact area between the pin and the disc and eliminate any difference in initial surface conditions between different pins. Both pin and disc surfaces were cleaned with ethyl alcohol and dried with airflow. Pin and disc masses were measured at the beginning and end of the tests in order to compare mass differences.

After pin-on-disc tests, the pins were embedded in bakelite, ground, polished and etched by a 2% Nital solution in order to analyze the wear sub-surface using a scanning electron microscope Inspect50 SEM-FEG. The microhardness variation of specimens as a function of distance from contact surface was obtained with HV0.05 using a durometer Shimadzu HMV-2TQDW.

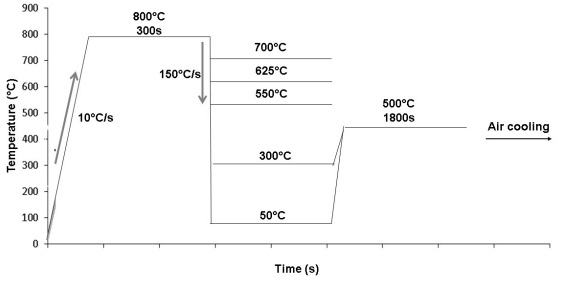

Figure 1. Heat treatment cycles.

3. Results and Discussion

3.1 Heat treatments and microstructures

Determination of critical temperatures is required to prevent the formation of undesirable microstructure and to optimize the efficiency of isothermal treatment, in some applications the presence of martensite is undesirable due to brittleness. Figure 2 presents the dilatometry curve obtained by experiment during heating and cooling rate

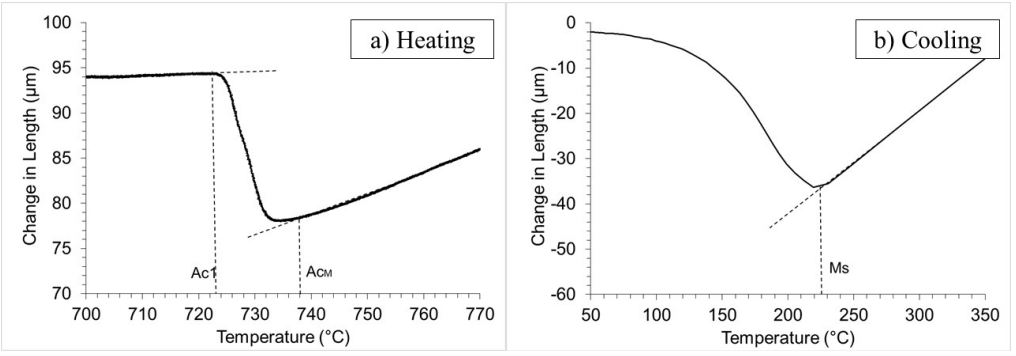

Figure 2. Dilatometry curve of a) heating and b) cooling.

Table 1. Chemical composition of the samples (wt. %).

C	S	Mn	P	Si	Al	N	CE
0.801	0.006	0.511	0.007	0.178	< 0.001	0.003	0.88

in 28°C/h and 150°C/s, respectively. During heating, the sample tends to present a linear expansion due to lattice parameter expansion. However, a large contraction appears in the dilatometry curve at Ac1 temperature in 723°C due to the beginning of eutectoid transformation. Partially ferrite and cementite dissolved in the austenite phase in this step. It is observed at 738°C eutectoid transformation was completed and austenite single-phase kept expanding with temperature increasing. During controlled rapid cooling, a drastic expansion happened at approximately 225°C due to austenite to martensite transformation ($\gamma_{FCC} \rightarrow 2\alpha_{BCC}$), indicates to the martensite start temperature (Ms).

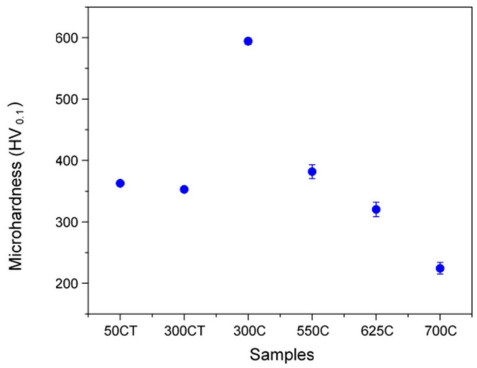

Figure 3. Microhardness of the specimens

The effect of different isothermal treatments on final microstructure was studied by SEM analyzing. The microhardness of specimens was shown in Figure 3. Figure 4 shows the micrographs of samples were subjected to the isothermal treatments and tempering (only 50CT and 300CT series). The interlamellar spacing of pearlite obtained were 243 ± 9 nm (700C sample), 128 ± 6 nm (625C sample) and 70 ± 4 nm (550C sample). Although the pearlitic microstructure was developed in three specimens (550C, 625C and 700C samples), continues increasing in the interlamellar spacing of pearlite was found as the increasing in isothermal temperature as predicted by Zener[19] in 1946. As expected, finer pearlite microstructure with less interlamellar spacing had the higher hardness values[4]. The 300C sample shows a lower bainitic microstructure (acicular ferrite plates with cementite particles precipitated inside them), the 300CT image reveals a tempered bainitic microstructure and 50CT tempered martensitic microstructure both with some spheroidizing cementite particles. Particles spheroidization can occur when steel is heated below eutectoid temperature for a long period of time.

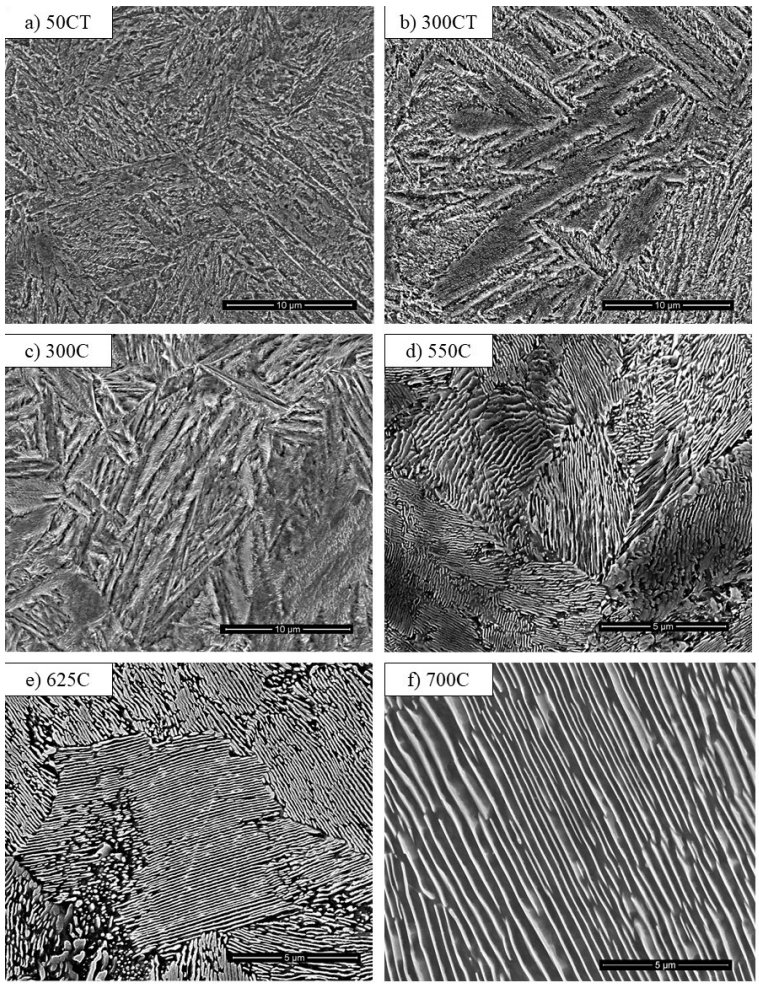

Figure 4. SEM micrographs of samples.

EBSD techniques as complementary method permits to determine crystal orientation and boundary properties. Figure 5 shows the transverse direction of inverse pole figure (IPF) map of transformed sample at 700°C. Color in IPF map indicates a particular crystal orientation, for instance green color corresponded the {110} planes parallel to the transverse direction (TD). The Figure 5 shows that ferrite grains orientated with {110} and {111} //TD are predominant in pearlite microstructure.

3.2 Mass loss and friction coefficient

Pin-on-disc test is widely used to investigate wear behavior due to various advantages such as short testing time, low costs, easy access and the possibility to obtain of different wear mechanisms[20]. Therefore, it was carried out for all samples studied in this work. The average of mass losses of pins and discs, wear rate per sliding distance and wear coefficient are listed in Table 2. In order to estimate the dimensionless wear coefficient (k) it was applied the "Archard wear equation"[21] indicates in the Equation 1. Q is the volume mass loss per unit of sliding distance, W is the normal load applied on the pin, L is the sliding distance and H is the hardness of softer surface. The wear coefficient must be dimensionless and it estimates the severity of slip wear[21]. The values of wear coefficient for each condition was illustrated in Figure 6.

$$Q = k * (W * L) / H \quad (1)$$

It is common the average of mass losses of pins is higher than discs. Straffelini et al.[22] reported that the temperature at pin surface has higher than the temperature at the disc surface. Thus, pin softening decreases wear resistance. It is also observed that the average mass loss of pins decreased with increasing in hardness and decreasing in interlamellar spacing. The sample transformed at 700°C showed a coefficient of wear 79% higher and lost three times more mass than the sample transformed at 500°C. This can be explained by decreasing the interlamellar spacing of pearlite and increasing the hardness.

The mass loss increases with hardness decreasing in almost all test conditions except in the 300C samples (lower bainite). These specimens have a higher hardness, but shows a significant pin mass loss. This behavior can be explained due remained martensitic structures, usually materials with untempered martensite microstructures are very fragile and have low wear resistance. The time that the samples 300C remained at 300°C not have been long enough to transform all austenite into bainite. Then, when these samples were air cooled, the remaining austenite was transformed in martensite.

The measurement of the coefficient of friction (μ) during the sliding test permits to characterize the behavior of the tribological mechanism. Moreover, it allows associate resistance to movement, breaking, and formation of oxide films and the changes and transitions of wear behavior[23]. The medium friction coefficients after the running in period were shown in the Figure 7.

The mass loss and coefficient of friction results demonstrated that wear resistance has an inverse correlation with an interlamellar spacing of pearlite. Pearlite microstructure transformed at the lower temperature, with less interlamellar

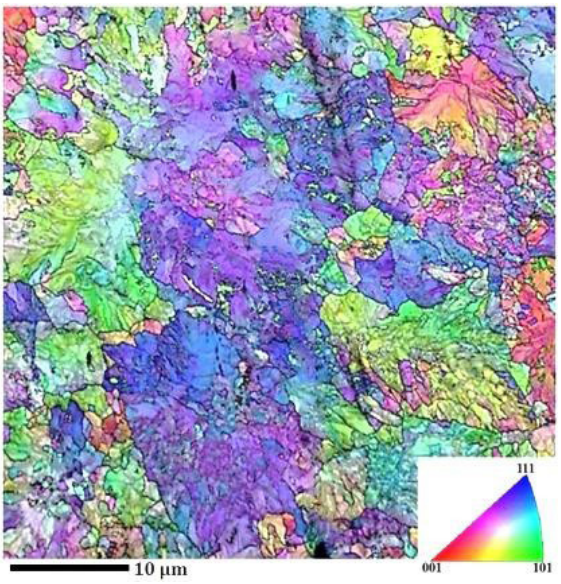

Figure 5. Transverse direction IPF of sample isothermally transformed at 700°C.

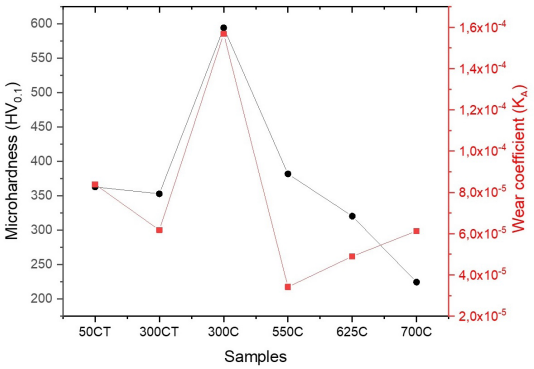

Figure 6. Microhardness and wear coefficient of specimens.

Table 2. Mass losses and wear coefficient of specimens.

Sample	Disc mass loss [mg]	Pin mass loss [mg]	Wear rate [mm³/m]	Wear coefficient (K_A)
50CT	0.8 ± 0.3	3.5 ± 0.8	0.24×10^{-3}	8.39×10^{-5}
300CT	1.3 ± 1.1	2.6 ± 0.5	0.19×10^{-3}	6.17×10^{-5}
300C	1.2 ± 0.5	3.9 ± 0.8	0.28×10^{-3}	15.68×10^{-5}
550C	0.6 ± 1.3	1.3 ± 0.3	0.09×10^{-3}	3.41×10^{-5}
625C	1.4 ± 1.3	2.3 ± 0.3	0.16×10^{-3}	4.89×10^{-5}
700C	0.9 ± 0.3	4.1 ± 1.1	0.29×10^{-3}	6.12×10^{-5}

spacing and greater hardness, exhibited the higher wear resistance. Temperature raising at pin surface during sliding increased fraction of oxides, consequently plays a significant role in wear behavior. Lewis and Dwyer-Joyce[24] reported that thermal softening leads to catastrophic accidents due to the large increase in wear rate.

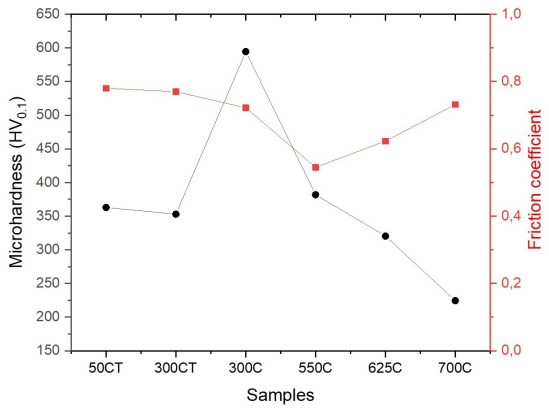

Figure 7. Friction coefficient after running in period in pin on disc tests.

The contaminants as well as uncontrollable environmental factors, including temperature and humidity, significantly affect wear performance during sliding operation[17,25]. Besides, oxide layers could also self-produce during the services due to friction can influence on the wear performance, the oxide layers avoid contact between the metal surfaces and generally maintains the system in mild wear regime.

3.3 Worn surfaces and strain hardening effects

Figure 8 presents the worn sub-surfaces of pins of different specimens after pin-on-disc test. It was observed in all samples a severe plastic deformation near to the contact surface. In pearlitic samples the cementite and ferrite lamella were aligned parallel to sliding direction in regions near to surface. The sample 300C presented the smallest thickness of plastic deformed layer.

The results show the severe deformation in sub-surface up to 10μm from surface which revealed a hardness increment from ~50±5% in sample subjected to isothermal treatment at 700°C to ~14±4% in sample subjected to isothermal treatment at 550°C, as a result of hardening of pearlite. This demonstrates that coarser pearlite with lower hardness had

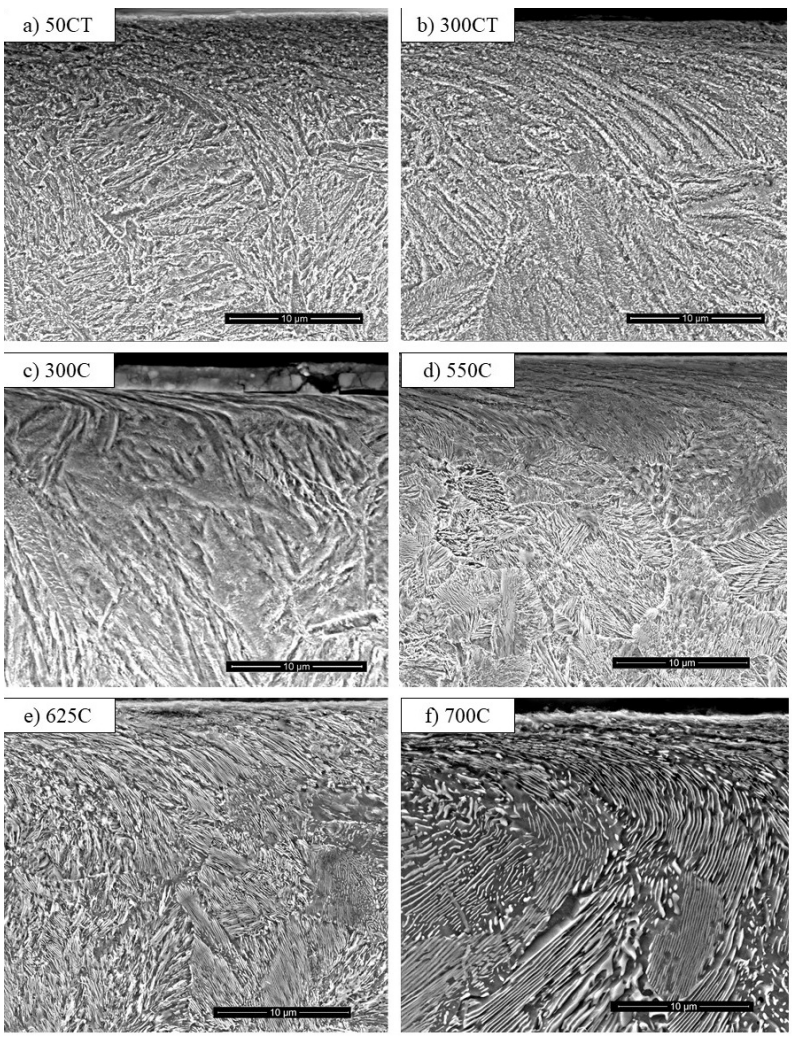

Figure 8. SEM micrographs of cross section pin samples.

the highest hardness increase rather than harder specimens. The microhardness variation of specimens as a function of distance from contact surface is indicated in the Figure 9. At 70 µm depth from surface, all the samples had hardness similar to undeformed microstructure.

3.4 EBSD – 700C samples analysis

In order to detailed study of deformed layer during sliding, EBSD analyze was carried out in this layer for 700C samples and shown in Figure 10a). IPF map was calculated by diffraction pattern (Kikuchi Pattern) following Bragg's diffraction conditions. Thus, it is expected that surface layer not be able to provide good quality of Kikuchi Pattern because of high number of dislocation densities. Image quality pattern of four different regions according the distance from surface are plotted in Figure 10b). It is observed that Region I which is located very close to the contact surface has the least image quality. However, image quality increases with increasing the distance from surface. This indicates the effect of a non-uniform deformation across thickness. As a result, excessive amount of dislocation tangles or pile-up dislocation in contact surface led to decreasing the quality of the Kikuchi pattern and image quality as well. There are some ultra-fine ferrite grains in district very close to the contact surface. The thermal reaction and thermal softening due to immense compressive force may enhance dislocation motion, besides decarburization leading to newly undeformed grains.

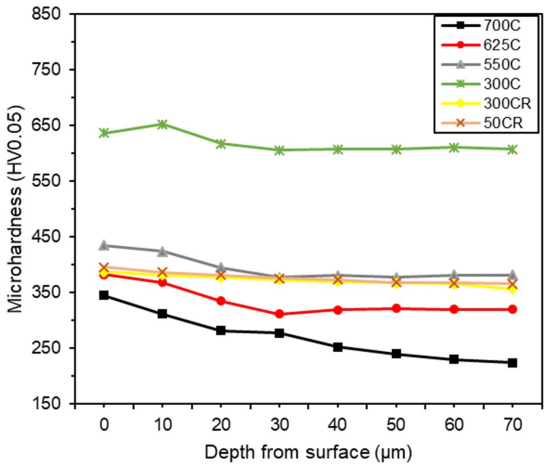

Figure 9. Microhardness profile of specimens as a function of distance from contact surface.

The variation of boundary types before pin-on-disc test and after according the different distance from surface are presented in Figure 11, this calculation was conducted with the same area of each region. Although these numbers cannot present the whole sample while it can show the tendency of dislocation distribution in different regions from contact surface. The very high fraction of random boundaries which greater than 15° misorientation between each point indicates the excessive dislocation densities in Region I. Then, fraction of HABs decreased gradually to reach the same amount of as-treated condition in about 40µm distance from surface. It could be concluded that the first 15µm area from the contact surface has suffered a severe deformation, while this deformation decreased up to 40µm to reach the same level of as-treated condition.

The crystallographic orientation in this IPF reveals that green ferrite grains related to {110} axis are predominant which corresponded to the most atomic dense plane in body-centered cubic (BCC). The variation of an individual grain which was drawn across thickness calculation in three depth of surface (i.e. a, b and c). The {110} pole figure map in these three points was plotted in Figure 12. Misorientation between a and b points was ~4.86°, while the deviation of a and c points reached about 14.86°. This also confirms the higher deformation concentration in a layer close the contact surface. The results obtained more evidence to occurrence of severe deformation in disc-pin contact region, which leading to deformation accumulation and excessive work hardening phenomenon. The results show the severe deformation in pin/disc contact led to formation of work-hardened layer with high accumulation of dislocation, which have a significant influence in wear rate.

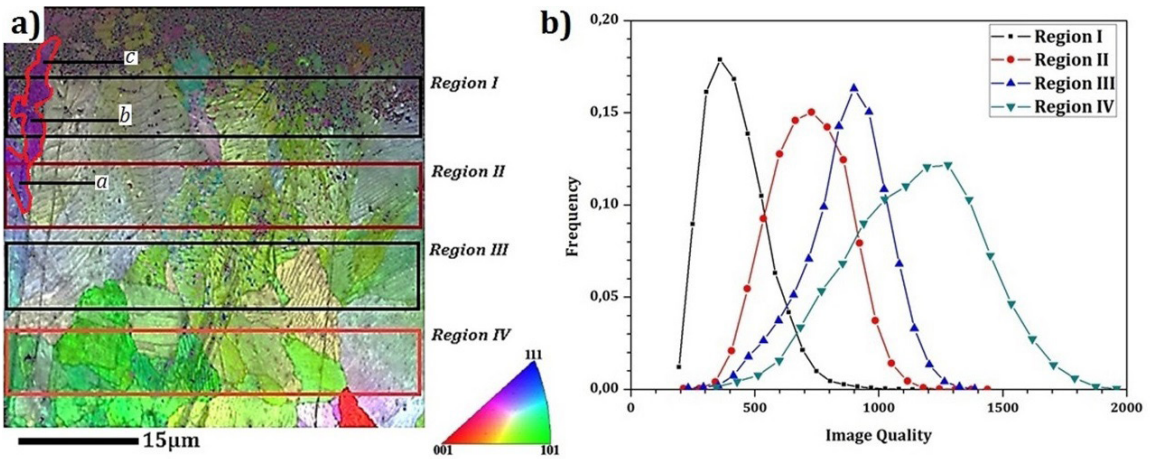

Figure 10. a) IPF color map and b) image quality index of worn surface sample transformed at 700°C after pin-on-disc test.

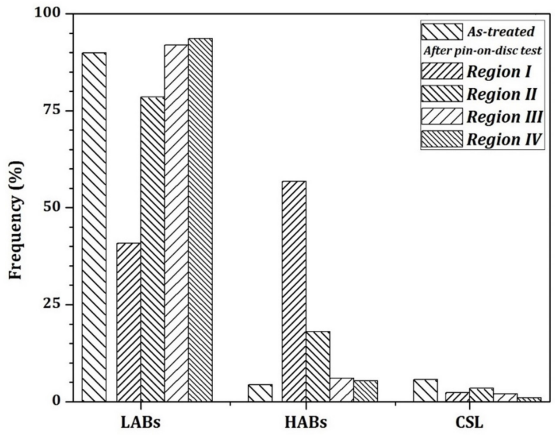

Figure 11. Boundary types distribution of specimens treated at 700°C before and after pin on disc tests.

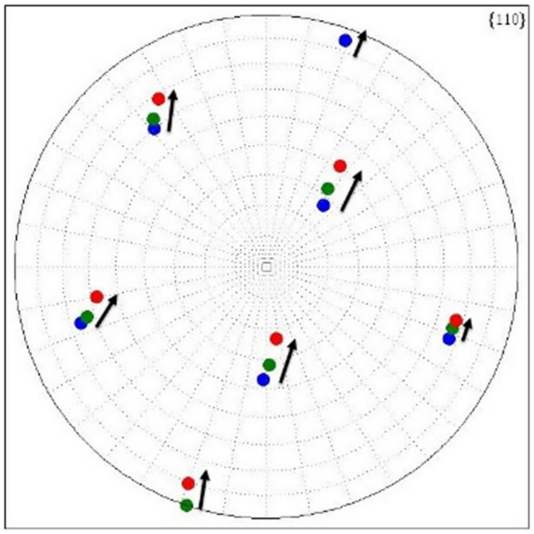

Figure 12. {110} pole figure of specimen treated at 700°C after pin on disc tests.

4. Conclusions

A detailed study of wear behavior of a pearlitic steel, corresponding to AAR class C railroad wheel steel, after isothermal treatment and tempering is a main interest of this work. The main conclusions of the study are summarized as follows:

- Fine pearlite shows superior sliding wear resistance than others structures analyzed in this work.
- The decrease in the pearlite formation temperature led to a reduction of the pearlite interlamellar spacing and to increased hardness.
- It was observed that the pearlite interlamellar spacing reduction promotes a better wear resistance performance in sliding wear tests.
- The severe deformation in sub-surface up to 10µm from surface significantly increases the hardness values.
- A non-uniform strain distribution in transverse direction can be detected from images obtained by Kikuchi pattern.
- Development of high angle boundaries in the region close to the contact surface is attributed to the formation of a work-hardened layer with high accumulation of dislocations.

5. Acknowledgments

The authors would like to thank CAPES, CNPq and VALE S.A. for the Wheel-Rail chair project and financial support

6. References

1. Aranda MM, Rementeria R, Poplawsky J, Urones-Garrote E, Capdevila C. The role of C and Mn at the austenite/pearlite reaction front during non-steady-state pearlite growth in a Fe–C–Mn steel. Scr Mater. 2015;104:67-70.
2. Wang M, Zhang F, Yang Z. Effects of high-temperature deformation and cooling process on the microstructure and mechanical properties of an ultrahigh-strength pearlite steel. Mater Des. 2017;114:102-10.
3. Chaves APG, Nishikawa LP, Goldenstein H, Padovese LR. The influence of pearlite lamellar distance on hardness, magnetic saturation and magnetic Barkhausen noise. In: ABM Week Congress; 2016; Rio de Janeiro - Brazil. Proceedings. São Paulo: ABM; 2016
4. Perez-Unzueta AJ, Beynon JH. Microstructure and wear resistance of pearlitic rail steels. Wear. 1993;164:173-82.
5. Singh UP, Singh R. Wear investigation of wheel and rail steels under conditions of sliding and rolling-sliding contact with particular regard to microstructural parameters. Wear. 1993;170:93-9.
6. Chaves APG. Railway wheels: analysis, microstructure and improvement proposals [dissertation]. São Paulo: Polytechnic School, University of São Paulo; 2017.
7. Chang LC. The rolling/sliding wear performance of high silicon carbide-free bainitic steels. Wear. 2005;258:730-43.
8. Bhadeshia HKDH. Bainite in steels: transformation, microstructure and properties. London: IOM Communications; 2001.
9. Leiro A, Kankanala A, Vuorinen E, Prakash B. Tribological behaviour of carbide-free bainitic steel under dry rolling/sliding conditions. Wear. 2011;273:2-8.
10. Viáfara CC, Castro MI, Vélez JM, Toro A. Unlubricated sliding wear of pearlitic and bainitic steels. Wear. 2005;259(6):405-11.
11. Liu JP, Li YQ, Zhou QY, Zhang YH, Hu Y, Shi LB, et al. New insight into the dry rolling-sliding wear mechanism of carbide-free bainitic and pearlitic steel. Wear. 2019;432-433:202943.
12. Hernández FCR, Demas NG, Davis DD, Polycarpou AA, Maal L. Mechanical properties and wear performance of premium rail steels. Wear. 2007;263:766-72.
13. Ball A. On the importance of work hardening in the design of wear-resistant materials. Wear. 1983;91:201-7.
14. Shipway PH, Wood SJ, Dent AH. The hardness and sliding wear behaviour of a bainitic steel. Wear. 1997;203(204):196-205.
15. Hasan SM, Chakrabarti D, Singh SB. Dry rolling/sliding wear behaviour of pearlitic rail and newly developed carbide-free bainitic rail steels. Wear. 2018;408(409):151-9.
16. Sethuramiah A, Kumar R. Modeling of chemical wear. Amsterdam: Elsevier; 2016. Chapter 3, Dry wear mechanisms and modeling, modeling of chemical; p. 41-68.
17. Hardwick C, Lewis R, Eadie DT. Wheel and rail wear: understanding the effects of water and grease. Wear. 2014;314(2):198-204.
18. Lyu Y, Zhu Y, Olofsson U. Wear between wheel and rail: A pin-on-disc study of environmental conditions and iron oxides. Wear. 2015;328:277-85.

19. Zener C. Phase transformations in steel. Trans Metall Soc AIME. 1946;167:550-95.
20. Lewis R, Olofsson U. Wheel-rail interface handbook. Burlington: Elsevier; 2009. Chapter 2, Basic tribology of the wheel-rail contact; p. 34-57.
21. Hutchings IM. Tribology: friction and wear of engineering materials. Cambridge: BH; 1992.
22. Straffelini G, Verlinski S, Verma PC, Valota G, Gialanella S. Wear and contact temperature evolution in pin-on-disc tribotesting of low-metallic friction material sliding against pearlitic cast iron. Tribol Lett. 2016;62:36-43.
23. Zum Gahr KH. Tribological aspects of microsystems. In: Fukuda T, Menz W, editors. Handbook of sensors and actuators. Amsterdam: Elsevier; 1998. Chapter 4; p. 83-113. vol. 6.
24. Lewis R, Dwyer-Joyce RS. Wear mechanisms and transitions in railway wheel steels. Proc Inst Mech Eng, Part J J Eng Tribol. 2005;218(6):467-78.
25. Abbasi S, Olofsson U, Zhu Y, Sellgren U. Pin-on-disc study of the effects of railway friction modifiers on airborne wear particles from wheel–rail contacts. Tribol Int. 2013;60:136-9.